STEM CELLS TRANSLATIONAL MEDICINE®

TISSUE ENGINEERING AND REGENERATIVE MEDICINE

Human Endomyocardial Biopsy Specimen-Derived Stromal Cells Modulate Angiotensin II-Induced Cardiac Remodeling

KAPKA MITEVA,[a,*] SOPHIE VAN LINTHOUT,[a,b,d,*] KATHLEEN PAPPRITZ,[a] IRENE MÜLLER,[a] FRANK SPILLMANN,[b] MARION HAAG,[a,c] HARALD STACHELSCHEID,[a] JOCHEN RINGE,[a,b] MICHAEL SITTINGER,[a,c] CARSTEN TSCHÖPE[a,b,d]

Key Words. Cardiac biopsy • Angiotensin II • Fibrosis • Cardiomyocyte hypertrophy

[a]Berlin-Brandenburg Center for Regenerative Therapies, [b]Department of Cardiology, and [c]Laboratory for Tissue Engineering, Charité, University Medicine Berlin, Campus Virchow, Berlin, Germany; [d]DZHK (German Center for Cardiovascular Research), Berlin, Germany

[*]Contributed equally.

Correspondence: Sophie Van Linthout, Ph.D., Berlin-Brandenburg Center for Regenerative Therapies, Föhrerstrasse 15, 13353 Berlin, Germany. Telephone: 49-(0)30-450539486; E-Mail: sophie.van-linthout@charite.de

Received January 16, 2016; accepted for publication June 13, 2016; published Online First on July 26, 2016.

1066-5099/2016/$20.00/0

http://dx.doi.org/10.5966/sctm.2016-0031

ABSTRACT

Cardiac-derived adherent proliferating cells (CardAPs) are cells derived from human endomyocardial biopsy specimens; they share several properties with mesenchymal stromal cells. The aims of this study were to evaluate whether intramyocardial injection of CardAPs modulates cardiac fibrosis and hypertrophy in a mouse model of angiotensin II (Ang II)-induced systolic heart failure and to analyze underlying mechanisms. Intramyocardial application of 200,000 CardAPs improved left ventricular function. This was paralleled by a decline in left ventricular remodeling, as indicated by a reduction in cardiac fibrosis and hypertrophy. CardAPs reduced the ratio of the left ventricle to body weight and cardiac myosin expression (heavy chain), and decreased the Ang II-induced phosphorylation state of the cardiomyocyte hypertrophy mediators Akt, extracellular-signal regulated kinase (ERK) 1, and ERK2. In accordance with the antifibrotic and antihypertrophic effects of CardAPs shown in vivo, CardAP supplementation with cardiac fibroblasts decreased the Ang II-induced reactive oxygen species production, α-SMA expression, fibroblast proliferation, and collagen production. Coculture of CardAPs with HL-1 cardiomyocytes downregulated the Ang II-induced expression of myosin in HL-1. All antifibrotic and antihypertrophic features of CardAPs were mediated in a nitric oxide- and interleukin (IL)-10-dependent manner. Moreover, CardAPs induced a systemic immunomodulation, as indicated by a decrease in the activity of splenic mononuclear cells and an increase in splenic CD4CD25FoxP3, CD4-IL-10, and CD8-IL-10 T-regulatory cells in Ang II mice. Concomitantly, splenocytes from Ang II CardAPs mice induced less collagen in fibroblasts compared with splenocytes from Ang II mice. We conclude that CardAPs improve Ang II-induced cardiac remodeling involving antifibrotic and antihypertrophic effects via paracrine actions and immunomodulatory properties. STEM CELLS TRANSLATIONAL MEDICINE *2016;5:1707–1718*

SIGNIFICANCE

Despite effective pharmacological treatment with angiotensin II type I receptor antagonists or angiotensin II-converting enzyme inhibitors, morbidity and mortality associated with heart failure are still substantial, prompting the search of novel therapeutic strategies. There is accumulating evidence supporting the use of cell therapy for cardiac repair. This study demonstrates that cells derived from human endomyocardial biopsies, cardiac-derived adherent proliferating cells (CardAPs), have the potential to reduce angiotensin II-induced cardiac remodeling and improve left ventricular function in angiotensin II mice. The mechanism involves antifibrotic and antihypertrophic effects via paracrine actions and immunomodulatory properties. These findings support the potential of CardAPs for the treatment of heart failure.

INTRODUCTION

Angiotensin (Ang) II is a key mediator in the pathogenesis of cardiac fibrosis and hypertrophy. In addition to its other effects, Ang II increases the deposition of the cardiac extracellular matrix by stimulating the proliferation of cardiac fibroblasts [1] and by the transdifferentiation of cardiac fibroblasts into myofibroblasts [2], it induces inflammation [3], and it stimulates the hypertrophic growth of cardiomyocytes [4], leading to cardiac remodeling and, consequently, left ventricular (LV) dysfunction and heart failure. Its importance in cardiac remodeling follows from animal studies [5, 6] and clinical trials [7] demonstrating that inhibition of Ang II by Ang II-converting enzyme (ACE) inhibitors or Ang II type I receptor (AT1R) antagonists prevents or reverses cardiac remodeling and

improves survival in patients with heart failure. However, despite effective pharmacological treatment with AT1R antagonists or ACE inhibitors, morbidity and mortality resulting from heart failure are still substantial, prompting the search of novel therapeutic strategies.

Mesenchymal stromal cells (MSCs) are well known for their immunomodulatory [8], proangiogenic [9], antiapoptotic [8], and antifibrotic features, and are an attractive cell source for cell therapy because of their low immunogenicity. To our knowledge, no studies are available that demonstrate direct antihypertrophic effects of MSCs on cardiomyocytes. We recently isolated and identified novel cardiac-derived cells from human endomyocardial biopsy specimens: cardiac-derived adherent proliferating cells (CardAPs) characterized as $CD105^+$, $CD73^+$, $CD166^+$, $CD44^+$, $CD90^-$, $CD14^-$, $CD34^-$, and $CD45^-$ [10, 11]. Similar to MSCs, CardAPs have antiapoptotic [12] and immunomodulatory [12, 13] features that they exert in a nitric oxide (NO)- and interleukin (IL)-10-dependent manner, and CardAPs also have low immunogenicity [13]. We previously demonstrated their cardioprotective potential in an experimental model of Coxsackievirus B3-induced myocarditis [12]. The aim of this study was to investigate whether CardAPs can modulate Ang II-induced cardiac fibrosis and hypertrophy in an experimental model of Ang II-induced heart failure and to analyze underlying mechanisms.

Materials and Methods

Cardiac-Adherent Proliferating Cell Isolation

Patients without symptoms and signs of congestive heart failure but suffering from atypical chest complaints underwent endomyocardial biopsy and right-side heart catheterization in a standardized manner [14] to exclude the existence of a cardiomyopathy after routine noninvasive diagnostic work-up and angiography had failed to elucidate any specific cause of heart failure. Cardiac adherent proliferating cells (CardAPs) were isolated from endomyocardial biopsy specimens taken from the right-ventricle side of the interventricular septum [15] of those patients ($n = 3$; age, 27 ± 2.1 years; male, $n = 2$; female, $n = 1$; ejection fraction: $63\% \pm 3.5\%$). Endomyocardial biopsy analysis excluded presence of relevant cardiotropic viruses and of prominent inflammation. CardAPs were harvested as described previously [10]. The donation of cardiac tissue was approved by the ethical committee of the Charité-Universitätsmedizin Berlin (No 225-07) and by the patients, who provided written consent.

Animals

To study the effect of CardAPs application on the progression of Ang II-induced heart failure, 2×10^5 CardAPs or phosphate-buffered saline (PBS) were intramyocardially injected in 8-week-old C57BL/6 mice, 1 week after implantation of osmotic pumps releasing Ang II (1.8 mg/kg body weight per day) [16] (n = 10–12 per group). Control mice received PBS instead of Ang II ($n = 8$ per group). Fourteen days after CardAPs application, hemodynamic parameters were analyzed, followed by harvesting of the left ventricle, which was next snap-frozen for molecular biology purposes and immunohistochemistry. For the analysis of T-regulatory cells (Tregs) and immunomodulatory mechanisms, spleens were isolated. To evaluate the engraftment of CardAPs after intramyocardial injection, the heart, spleen, lung, kidney, and liver were harvested. The investigation was performed in accordance with the principles of laboratory animal care and the German law on animal protection, and was approved by the ethical committee for the use of experimental animals of the Charité-Universitätsmedizin Berlin (No. g0094/01).

Assessment of CardAP Engraftment

The engraftment of CardAPs in the heart, lung, kidney, liver, and spleen after intramyocardial application was determined according to the method of McBride et al. [17], slightly modified, as described previously [12]. In brief, genomic DNA was extracted from frozen tissues as described previously [18]. A standard curve was generated using human genomic DNA obtained from human umbilical vein endothelial cells serially diluted over a 100,000-fold dilution range into murine spleen genomic DNA. Real-time polymerase chain reaction (PCR) was performed with 800 ng of target DNA, *Alu* specific primers, and a fluorescent probe [17]. Values are expressed as a percentage of human DNA per 800 ng of murine tissue.

Real-Time PCR

RNA was isolated from the left ventricle using the RNeasy Mini Kit according to the manufacturer's protocol (Qiagen, Hilden, Germany, https://www.qiagen.com), followed by cDNA synthesis. Quantitative real-time PCR (Mastercycler ep gradient realplex; Eppendorf, Hamburg, Germany, http://www.eppendorf.com) was performed to assess the LV mRNA expression of the target genes *Col I* and *Col III*, using gene expression assays for Col1a1 Mm01302043_g1, Col3a1 Mm00802331_m1 (Thermo Fisher Scientific Life Sciences, Waltham, MA, http://www.thermofisher.com). For the analysis of LV IL-10 mRNA expression, the forward primer 5′-GCCCCAGGCAGAGAAGCATGG-3 and reverse primer 5′-GGGAGAAATCGATGACAGCGCCT-3′ (TIB MOLBIOL, Berlin, Germany, http://www.tib-molbiol.com) were used, combined with Sybr Green (Thermo Fisher Scientific Life Sciences). mRNA expression was normalized to the housekeeping gene *18S* and relatively expressed with the control group set as 1.

Cell Culture

Human CardAPs were cultured at a density of 6,000 cells/cm^2 in medium consisting of equal proportions of Iscove's Modified Dulbecco's Medium/Dulbecco's modified Eagle's medium /Ham's F-12 medium (Biochrom, Berlin, Germany, http://www.biochrom.de) containing 5% human serum, 1% penicillin/streptomycin, 20 ng/ml basic fibroblast growth factor (Peprotech, Hamburg, Germany, https://www.peprotech.com), and 10 ng/ml epithelial growth factor (Peprotech). Human cardiac fibroblasts were cultured in Lung/Cardiac Fibroblasts Basal Medium (Cell Applications, San Diego, CA, https://www.cellapplications.com) plus supplements (Cell Applications). Murine HL-1 cells were cultured in Claycomb medium (Sigma-Aldrich, Lenexa, KS, http://www.sigmaaldrich.com) supplemented with 10% fetal bovine serum (FBS), 1% penicillin/streptomycin, 100 μM norepinephrine (Sigma-Aldrich), and 2 mM glutamine.

Coculture of Cardiac Fibroblasts With Endomyocardial Biopsy Specimen-Derived Cells

Human cardiac fibroblasts were plated at a cell density of 135,000 cells per 6-well, 10,000 cells per 96-well, or 10,000 cells per 8-well chamber slide. After 24 hours of culture, human cardiac

fibroblasts were stimulated with Ang II at a concentration of 1 μM. Four hours after Ang II stimulation, untreated CardAPs, or CardAPs pretreated for 24 hours with 10 mM nitro-L-argininmethylesterhydrochloride (L-NAME; Sigma-Aldrich) were collected and added to the human cardiac fibroblasts for coculture at a ratio of 1 CardAP to 10 human cardiac fibroblasts. To investigate whether CardAPs mediate their effects via IL-10, 1 μg/ml anti-human IL-10 antibody was added at the time point of CardAP supplementation.

Cocultures of cardiac fibroblasts with CardAPs were performed to evaluate the impact of CardAPs on the Ang II-induced cardiac fibroblast collagen I and III production (collagen I and III staining, Sirius Red staining), fibroblast proliferation, the transdifferentiation of cardiac fibroblasts into myofibroblasts via the analysis of α-SMA expression, and on the induction of oxidative stress in cardiac fibroblasts. Oxidative stress in human cardiac fibroblasts was evaluated by flow cytometry via the analysis of reactive oxygen species (ROS) by 5- (and 6-) chloromethyl-2′,7′-dichlorodihydrofluorescein diacetate, acetyl ester (CM-H_2DCFDA; Thermo Fisher Scientific Life Sciences).

Collagen I and III Staining

Human cardiac fibroblasts were cultured at a density of 10,000 cells per well in fibronectin-coated 8-well Laboratory Tek Chamber slides (Thermo Fisher Scientific Life Sciences; fibronectin from Sigma-Aldrich), stimulated with Ang II at a concentration of 1 μM, and subsequently cocultured with DiO-labeled CardAPs (Vybrant DiO Cell-labeling solution; Thermo Fisher Scientific Life Sciences), as described previously in Materials and Methods. After 24 hours of Ang II stimulation, human cardiac fibroblasts were washed with PBS and fixed in 4% paraformaldehyde for 10 minutes at room temperature (RT). Blocking was performed in PBS containing 3% bovine serum albumin (BSA; Sigma-Aldrich) and 0.05% Tween 20 (Sigma-Aldrich) for 30 minutes at RT, followed by a 1-hour incubation at RT with rabbit polyclonal collagen I or III antibody diluted 1:100 (Abcam, Cambridge, U.K., http://www.abcam.com) in blocking solution. After washing with PBS, incubation with a goat anti-rabbit-Cy3 secondary antibody (Thermo Fisher Scientific Life Sciences) diluted 1:2,000 was performed at RT for 1 hour. Mounting medium (Vector Laboratories, Burlingame, CA, https://vectorlabs.com) with 4′,6-diamidino-2-phenylindole (DAPI; Sigma-Aldrich) diluted 1:1,000 was added and cover slips were mounted on the microscopy slides. Images were acquired on a Zeiss Axio Observer Z1 microscope (Zeiss International, Oberkochen, Germany, http://www.zeiss.com), using AxioVision Rel 4.7 imaging software (Zeiss International). Representative pictures show a merged image of the cocultured DiO-labeled CardAPs with Ang II-stimulated cardiac fibroblasts stained for Cy3-collagen I or III, and DAPI.

CFSE Proliferation Assay of Human Cardiac Fibroblasts

Human cardiac fibroblasts were labeled with 10 μM succinimidyl ester of carboxyfluorescein diacetate (CFSE Cell Tract; Thermo Fisher Scientific Life Sciences), stimulated with Ang II at a concentration of 1 μM, and subsequently cocultured with untreated CardAPs or L-NAME-pretreated CardAPs in the presence or absence of 1 μg/ml anti-human IL-10 antibody, as described above. All samples were acquired on FACS BD FACSCanto II with BD FACSDiva software version 6.1.3 (BD Biosciences, Franklin Lakes, NJ, http://www.bdbiosciences.com). Reanalysis of fluorescence-activated cell sorting (FACS) data was performed using FlowJo software version 8.8.6 (Tree Star, Ashland, OR, http://www.flowjo.com). Finally, the average number of cell divisions that the responding cells underwent, excluding the cells of peak 0 that did not divide, were calculated by the software as the division index.

Intracellular α-Smooth Muscle Actin Staining

DiO-labeled (Vybrant DiO Cell-labeling solution; Thermo Fisher Scientific Life Sciences) human cardiac fibroblasts were stimulated with Ang II and subsequently cocultured with CardAPs, as described previously in Materials and Methods. After 24 hours of Ang II stimulation at a concentration of 1 μM in the presence or absence of CardAPs, human cardiac fibroblasts were fixed in fixation/permeabilization solution (BD Cytofix/Cytoperm Plus Fixation/Permeabilization Kit; BD Biosciences) and stained with α-SMA-PE antibody. All the samples were acquired on FACS BD FACSCanto II with BD FACSDiva software version 6.1.3 (BD Biosciences). Reanalysis of FACS data was performed using FlowJo software version 8.8.6 (Tree Star). Data are presented as DiO^+/α-SMA-PE^+ cells (percentage of gated).

Reactive Oxygen Species Analysis

Dil-labeled (Vybrant Dil Cell-labeling solution; Thermo Fisher Scientific Life Sciences) human cardiac fibroblasts were stimulated with Ang II at a concentration of 1 μM and subsequently cocultured with CardAPs, as described previously in Materials and Methods. After stimulation with Ang II for 24 hours, cells were collected in prewarmed PBS containing 5 μM CM-H_2DCFDA, and then incubated at 37°C for 30 minutes. After washing with PBS, all the samples were analyzed by flow cytometry (BD FACSCantoII, BD FACSDiva software 6.1.3; BD Biosciences). Reanalysis of FACS data was performed using FlowJo software version 8.8.6 (Tree Star). Data are represented as Dil^+/DCF^+ cells (percentage of gated).

Flow Cytometry Analysis of Spleen Mononuclear Cells

Splenocytes were isolated from control, Ang II, and Ang II CardAPs mice, slightly modifying the method of De Geest et al. [19]. Flow cytometry analysis of spleen mononuclear cells (MNCs) was performed using anti-mouse IL-10 in BD Perm/Wash solution (BD Biosciences) according to the manufacturer's instructions. The mouse Treg detection kit containing CD4, CD25, and FoxP3 antibodies, and fixation and wash solutions was purchased from Miltenyi Biotec (Bergisch Gladbach, Germany, http://www.miltenyibiotec.com). Surface staining was performed according to the manufacturer's instructions. Splenocytes were first stained with anti-mouse CD4 and CD25 antibodies; after fixation, intracellular FoxP3 staining was performed. Spleen MNCs were labeled with 10 μM succinimidyl ester of carboxyfluorescein diacetate (CFSE Cell Tract; Thermo Fisher Scientific Life Sciences) to be able to measure cell proliferation indicative of spleen MNC activation. Sample analysis was performed on a MACSQuant Analyzer (Miltenyi Biotec). Reanalysis of FACS data was performed using FlowJo software version 8.8.6 (Tree Star).

Coculture of Fibroblasts With Splenic Cells

Murine C4 fibroblasts were plated at a cell density of 10,000 cells per 96-well chamber slide in Basal Iscove medium (Biochrom) supplemented with 10% FBS and 1% penicillin/streptomycin. Twenty-four hours after plating, the medium was removed and

splenic cells isolated from control, Ang II, and Ang II CardAP mice were added to the fibroblasts at a ratio of 10 splenic cells to 1 fibroblast in Roswell Park Memorial Institute medium (Thermo Fisher) 10% FBS, and 1% penicillin/streptomycin, and activated with 50 ng/ml phorbolmyristate acetate (PMA) and 500 ng/ml ionomycin. After 3 days, the splenic cells were removed and Sirius Red staining was performed.

Sirius Red Staining

Sirius Red staining of murine fibroblasts was performed as described previously [21]. In brief, murine C4 fibroblasts were fixed in methanol overnight at −20°C, washed once with PBS, and incubated in 0.1% Sirius Red staining solution at RT for 1 hour. After a second wash with PBS, the Sirius Red staining of the fibroblasts was eluted in 0.1 N sodium hydroxide at RT for 1 hour on a rocking platform. The optical density, representative of the accumulation of collagen I and III, was measured at 540 nm on a SpectraMax 340PC microplate reader (Molecular Devices, Munich, Germany, https://www.moleculardevices.com).

Western Blotting

Left ventricle samples were homogenized in lysis buffer (Thermo Fisher Scientific Life Sciences) supplemented with proteinase inhibitors (F. Hoffmann-La Roche, Basel, Switzerland, http://www.roche.com). An equal amount of protein was loaded into 10%–12% SDS-polyacrylamide gels. Total and *p*-Akt, -ERK1, -ERK2 (Cell Signaling Technology, Danvers, MA, http://www.cellsignal.com), myosin (Abcam), β tubulin (Santa Cruz Biotechnology, Santa Cruz, CA, http://www.scbt.com), and glyceraldehyde-3-phosphate dehydrogenase (GAPDH; BPS Bioscience, San Diego, CA, http://bpsbioscience.com) were detected with each specific antibody, followed by incubation with an IRdye secondary antibody (LI-COR Biosciences, Lincoln, NE, https://www.licor.com). The blots were visualized with Odyssey (LI-COR Biosciences). Quantitative analysis of the intensity of the bands was performed with Odyssey V3.0 software.

Sarcomeric Myosin Heavy Chain Flow Cytometry

Dil-labeled HL-1 cardiomyocytes were plated at a density of 200,000 cells per 6-well chamber slide. After 24 hours of culture, HL-1 cells were stimulated with 1 μM Ang II. Four hours after Ang II supplementation, untreated CardAPs, or CardAPs pretreated for 24 hours with 10 mM of L-NAME (Sigma-Aldrich) were collected and added to the HL-1 cells for coculture at a ratio of 1 CardAP to 10 HL-1 cells. To investigate whether CardAPs mediate their effects via IL-10, 1 μg/ml anti-human IL-10 antibody was added at the time point of CardAP supplementation. After 24 hours of Ang II stimulation, HL-1 cells were fixed and permeabilized with fixation/permeabilization solution (BD Cytofix/Cytoperm Plus Fixation/Permeabilization Kit; BD Biosciences) and stained with antimyosin heavy chain Alexa Fluor 488 (eBioscience, San Diego, CA, http://www.ebioscience.com) for 30 minutes at RT. All the samples were acquired on FACS BD FACSCanto II with BD FACSDiva software version 6.1.3 (BD Biosciences). Reanalysis of FACS data was performed using FlowJo software version 8.8.6 (Tree Star). Data are presented as myosine$^+$/Dil$^+$ cells (percentage of gated).

Sarcomeric Myosin Heavy Chain Immunostaining

HL-1 cells were plated in CellCarrier-96 Black Optically Clear Bottom 96-well plates (PerkinElmer, Greenville, SC, http://www.perkinelmer.com), stimulated with 1 μM Ang II, and cocultured with Dil-labeled CardAPs. Twenty-four hours after Ang II supplementation, cells were washed with PBS, fixed and permeabilized with the fixation/permeabilization solution, then incubated for 1 hour at RT with the MF-20 antibody (Developmental Studies Hybridoma Bank, Iowa City, IA, http://dshb.biology.uiowa.edu/) and 45 minutes of incubation at RT with the secondary Cy5 antibody (Thermo Fisher Scientific Life Sciences) in PBS plus 1% BSA and 0.2% Triton-X. Finally, cells were stained with DAPI (Sigma-Aldrich) diluted 1:1,000 in PBS. The images were acquired on Operetta High Content Imaging System with Harmony High Content Imaging and Analysis Software (PerkinElmer).

Hemodynamic Measurements

Fourteen days after intramyocardial injection of CardAPs, mice were anesthetized (0.8–1.2 g/kg urethane and 0.05 mg/kg buprenorphine intraperitoneally) and artificially ventilated. A 1.2F microconductance pressure-volume catheter (Transconic Scisense, London, ON, Canada, http://www.transonic.com) was positioned in the left ventricle through the apex for continuous registration of LV pressure-volume loops in an open chest model [8]. The volumes were calibrated using the hypertonic saline technique [22]. All measurements were performed three times while ventilation was turned off momentarily. Indices of systolic and diastolic cardiac performance were derived from LV pressure-volume data obtained at steady state. Heart rate (HR), left ventricle contractility (dP/dt_{max}), LV pressure decrease (dP/dt_{min}.), stroke volume, stroke work, end-systolic volume (ESV) and end-diastolic volume (EDV), LV relaxation time (τ), LV end-diastolic pressure (LVEDP), ejection fraction (EF), and cardiac output (CO) as indices of LV systolic and diastolic function were recorded.

Statistical Analysis

Statistical analysis was performed using Prism 6 for Mac OS X (GraphPad Software, La Jolla, CA, http://www.graphpad.com). Ordinary one-way analysis of variance was used for statistical analysis of the data. Data are presented as mean ± SEM. Differences were considered to be significant when the two-sided *p* value was less than .05.

RESULTS

Engraftment of Endomyocardial Biopsy Specimen-Derived Cells After Intramyocardial Application

Two weeks after intramyocardial application of 2×10^5 CardAPs, CardAPs could be retrieved in the murine organs, as confirmed by human *Alu* detection via real-time PCR (Fig. 1). The engraftment in the heart was 2.7-fold, 3.3-fold, 3.2-fold, and 3.3-fold higher than in the lung, kidney, liver, and spleen, respectively ($p < .05$).

Endomyocardial Biopsy Specimen-Derived Cells Reduced Cardiac Fibrosis in Angiotensin II-Treated Mice

Given the importance of Ang II in the induction of cardiac fibrosis [23] on the one hand and the well-described antifibrotic effects of MSCs on the other hand [24], we investigated whether MSC-like CardAPs were also able to reduce cardiac fibrosis in Ang II-treated

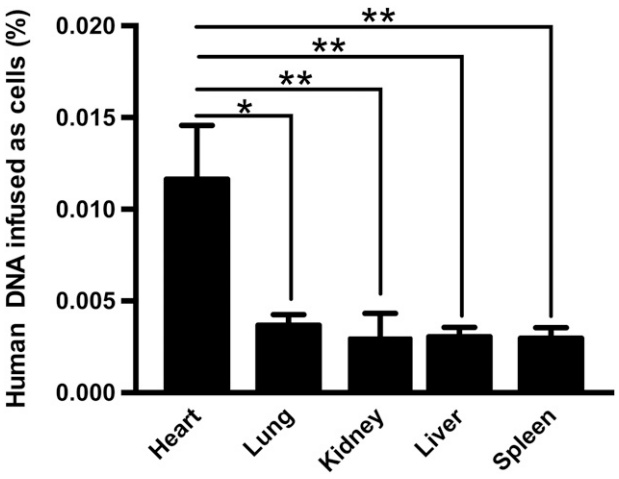

Figure 1. Engraftment of endomyocardial biopsy specimen-derived cells after intramyocardial injection. Bar graphs represent the percentage of human DNA infused as cells in the heart, lung, kidney, liver, and spleen of angiotensin II-treated mice intramyocardially injected with cardiac-derived adherent proliferating cells. $n = 3–4$ per group. *, $p < .05$; **, $p < .01$ versus heart.

mice. Ang II induced cardiac fibrosis as indicated by a 2.8- and 2.7-fold increase in LV collagen I and III mRNA expression, respectively ($p < .001$ vs. control mice), whereas CardAPs application in Ang II mice decreased LV Col I and Col III mRNA expression by 1.6- and 1.8-fold, respectively ($p < .01$ vs. Ang II mice) (Fig. 2A).

Endomyocardial Biopsy Specimen-Derived Cells Exerted Direct Antifibrotic Effects

Because the expression levels of the AT1R define the biological efficacy of Ang II [25], we first analyzed whether CardAPs affect the expression of AT1R in cardiac fibroblasts. CardAPs diminished the Ang II-mediated upregulation of the AT1R in cardiac fibroblasts by 3.6-fold ($p < .0001$) (Fig. 2B). After this finding, we further analyzed the antifibrotic effects of CardAPs and whether they occurred similar to their antiapoptotic [12], antiviral [12], and immunomodulatory [12] properties in an NO- and/or IL-10-dependent manner. Therefore, basal and Ang II-stimulated cardiac fibroblasts were cocultured with untreated or L-NAME-treated CardAPs or CardAPs in the presence of an anti-human IL-10 antibody. Collagen I and III immunostaining showed that CardAPs reduced the Ang II-induced collagen I and III production in cardiac fibroblasts (Fig. 2C: upper panel, Col I; lower panel, Col III). Similarly, Sirius Red staining demonstrated that CardAPs decreased the Ang II-promoted collagen accumulation by 1.3-fold ($p < .01$; Fig. 2D). In addition, cardiac fibroblast proliferation was 1.9-fold ($p < .0001$) lower in Ang II-stimulated cardiac fibroblasts cocultured with CardAPs compared with Ang II-stimulated monocultured cardiac fibroblasts (Fig. 3A). Besides the CardAPs-mediated decrease in collagen production and proliferation of Ang II-stimulated cardiac fibroblasts, CardAPs also reduced the transdifferentiation of cardiac fibroblasts into myofibroblasts, as indicated by a 1.9-fold ($p < .0001$) reduction in α-SMA expression (Fig. 3B). Finally, given the importance of the intracellular oxidation status for cardiac fibrosis [23, 26], we analyzed whether CardAPs supplementation to Ang II-stimulated cardiac fibroblasts could affect ROS production. Coculture of CardAPs with Ang II-stimulated cardiac fibroblasts resulted in a 3.0-fold reduction ($p < .0001$ vs. Ang II) in ROS production (Fig. 3C). All CardAPs-mediated effects were blunted in the presence of L-NAME or by blocking human IL-10, suggesting that the antifibrotic effects of CardAPs were mediated in an NO- and IL-10-dependent manner.

Endomyocardial Biopsy Specimen-Derived Cells Exhibited Prominent Immunomodulatory Effects, Which Affected Collagen Production in Fibroblasts

Because Ang II mediates key events of inflammatory processes [27] on the one hand and CardAPs are known for their immunomodulatory properties [12, 13] on the other hand, we next explored the immunomodulatory effects of CardAPs in Ang II-treated mice. These mice exhibited significantly lower MNC activation and proliferation, as indicated by a 1.3-fold lower division index compared with spleen MNCs of Ang II mice ($p < .01$) (Fig. 4A). Moreover, CardAP injection in Ang II mice resulted in a 1.7-fold increase in the percentage of Tregs ($p < .05$ vs. Ang II mice) (Fig. 4B), which was accompanied by a 1.8-fold elevation in the percentage of immunoregulatory IL-10-producing CD4 and CD8 cells ($p < .05$ and $p < .001$ vs. Ang II mice, respectively; Fig. 4C) [28]. In parallel, CardAPs raised LV *IL-10* mRNA expression in Ang II mice 5.2-fold ($p < .05$ vs. Ang II mice) (control mice, 1 ± 0.17; Ang II mice, 1.2 ± 0.29; Ang II CardAPs mice, 6.2 ± 2.6; $n = 5$ per group).

Given the link between inflammation and cardiac fibrosis' [20, 29], we further investigated whether the reduction in cardiac fibrosis in Ang II CardAPs mice compared with Ang II mice could partly be mediated via the immunomodulatory effects of CardAPs. Therefore, splenocytes from the different experimental groups were cocultured with fibroblasts and their impact on collagen production verified. Supplementation of splenocytes from Ang II CardAPs mice induced 2.1-fold ($p < .0001$) less collagen production in fibroblasts compared with splenocytes isolated from Ang II mice (Fig. 4D), suggesting an impact of the CardAP-mediated immunomodulatory effects on cardiac fibrosis in Ang II mice.

Endomyocardial Biopsy Specimen-Derived Cells Reduced Cardiac Hypertrophy

In parallel with the decrease in cardiac fibrosis, CardAPs also reduced the Ang II-induced cardiac hypertrophy as indicated by a 1.2-fold ($p < .01$) and 2.8-fold ($p < .0001$) decline in left ventricle to body weight ratio and cardiac myosin (heavy chain) expression, respectively (Fig. 5A, 5B). Concomitantly, CardAPs decreased the Ang II-promoted phosphorylation state of the cardiomyocyte hypertrophy mediators ERK1, ERK2, and Akt, by 1.4-fold ($p < .01$), 1.2-fold ($p < .05$), and 1.9-fold ($p < .001$) versus Ang II mice, respectively (Fig. 5C, 5D).

Endomyocardial Biopsy Specimen-Derived Cells Mediated Direct Antihypertrophic Effects

To evaluate whether CardAPs could directly affect cardiomyocyte hypertrophy, CardAPs were cocultured with Ang II-treated HL-1 cardiomyocytes. CardAP supplementation to Ang II-stimulated cardiomyocytes resulted in a visual reduction of the intensity of myosin compared with Ang II-stimulated HL-1 cells cultured in the absence of CardAPs (Fig. 6A). This finding was supported by the 3.3-fold ($p < .0001$) lower percentage of $Dil^+/Myosin^+$ positive HL-1 cells present in Ang II HL-1 CardAPs cocultures versus Ang II HL-1 monocultures. All CardAPs-mediated effects were blunted in the presence of L-NAME or by blocking human IL-10, suggesting that the antihypertrophic effects of CardAPs were mediated in an NO- and IL-10-dependent manner (Fig. 6B).

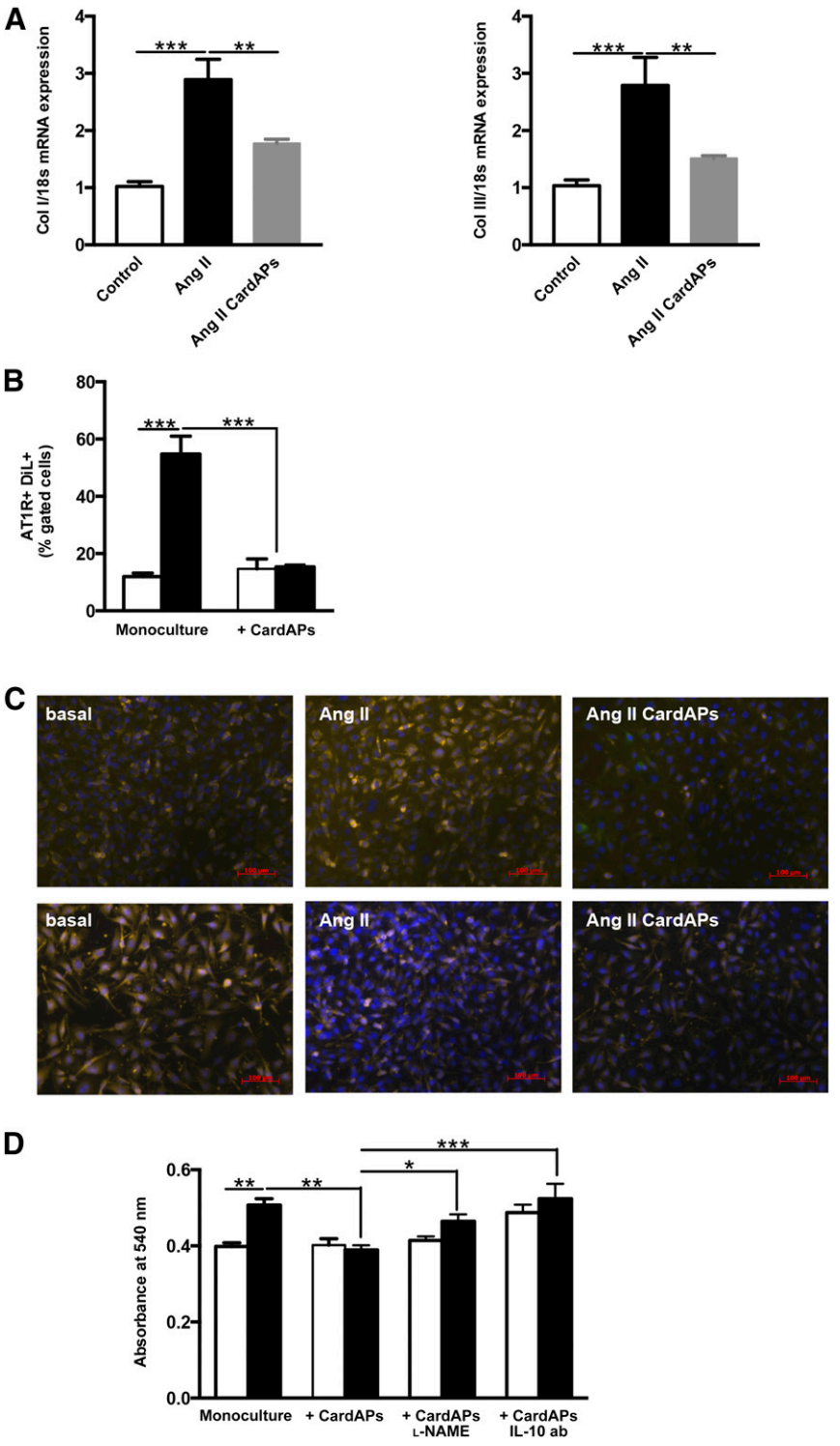

Figure 2. Endomyocardial biopsy specimen-derived cells reduced cardiac fibrosis in Ang II-treated mice and decreased Ang II-induced cardiac fibroblast collagen production in a nitric oxide- and IL-10-dependent manner. **(A):** Bar graphs represent the mean ± SEM of Col I and Col III mRNA expression in the left ventricle of control, Ang II, and Ang II CardAPs mice, as indicated. $n = 6–8$ per group. **, $p < .01$; ***, $p < .001$. **(B):** Bar graphs represent the mean ± SEM of $AT1R^+/DiI^+$ cells depicted as the percentage of gated cells of basal (open bars) or Ang II-treated (closed bars) cardiac fibroblasts with or without CardAPs. $n = 4$ per group. ***, $p < .001$. **(C):** Upper and lower panels present representative pictures of Col I- and Col III-stained cardiac fibroblasts, respectively, which were stimulated with Ang II in the presence or absence of CardAPs, as indicated. Pictures are merged images of Col I/III-, 4′,6-diamidino-2-phenylindole, and/or DiO-labeled CardAPs at magnification ×20. **(D):** Bar graphs represent the mean ± SEM of the absorbance at 540 nm of Sirius Red-stained basal (open bars) or Ang II-treated (closed bars) cardiac fibroblasts with or without untreated or L-NAME-treated CardAPs or CardAPs in the presence of 1 μg/ml anti-human IL-10 ab, as indicated. $n = 4–6$ per group. *, $p < .05$; **, $p < .01$; ***, $p < .001$. Abbreviations: ab, antibody; Ang, angiotensin; AT1R, angiotensin II type I receptor; CardAP, cardiac-derived adherent proliferating cell; IL, interleukin; L-NAME, nitro-L-argininmethylesterhydrochloride.

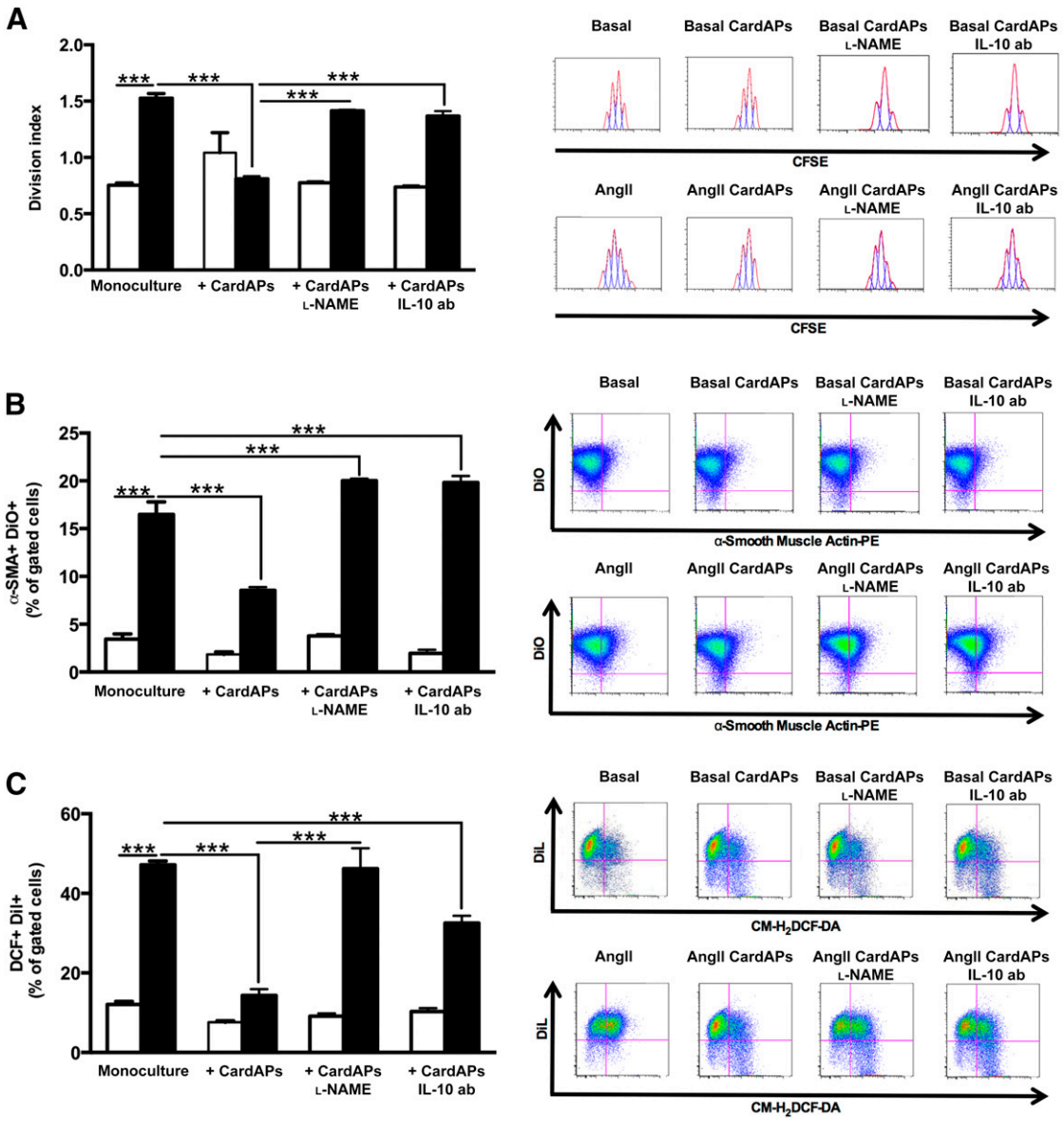

Figure 3. Endomyocardial biopsy specimen-derived cells diminished Ang II-induced cardiac fibroblast proliferation, transdifferentiation into myofibroblasts, and oxidative stress in a nitric oxide- and IL-10-dependent manner. **(A):** Left panel represents bar graphs depicting the mean ± SEM of the division index of basal (open bars) or Ang II-treated (closed bars) cardiac fibroblasts with or without untreated or L-NAME-treated CardAPs or CardAPs in the presence of 1 μg/ml anti-human IL-10 antibody. $n = 4$ per group. ***, $p < .001$. Right panel shows peaks indicating the amount of cell divisions in the respective condition. **(B):** Left panel shows bar graphs representing the mean ± SEM of α-SMA$^+$/DiO$^+$ cells, depicted as the percentage of gated cells of basal (open bars) or Ang II-treated (closed bars) cardiac fibroblasts with or without untreated or L-NAME-treated CardAPs or CardAPs in the presence of 1 μg/ml anti-human IL-10 ab. $n = 4$ per group. ***, $p < .001$. The right panel represents dot plots of α-SMA$^+$/DiO$^+$ cells, as indicated. **(C):** Left panel demonstrates bar graphs representing the mean ± SEM of DCF$^+$/DiI$^+$ cells, depicted as the percentage of gated cells of basal (open bars) or Ang II-treated (closed bars) cardiac fibroblasts with or without untreated or L-NAME-treated CardAPs or CardAPs in the presence of 1 μg/ml anti-human IL-10 ab. $n = 4$ per group. ***, $p < .001$. The right panel illustrates representative dot plots of DCF$^+$/DiI$^+$ cells of the respective conditions. Abbreviations: ab, antibody; Ang, angiotensin; CardAP, cardiac-derived adherent proliferating cell; CFSE, succinimidyl ester of carboxyfluorescein diacetate; CM-H_2DCFDA, chloromethyl-2′,7′-dichlorodihydrofluorescein diacetate, acetyl ester; IL, interleukin; L-NAME, nitro-L-argininmethylesterhydrochloride; PE, phycoerythrin.

Endomyocardial Biopsy Specimen-Derived Cells Improved Left Ventricular Function in Angiotensin II-Treated Mice

Finally, we evaluated whether the CardAP-mediated modulation of cardiac remodeling was associated with an improvement in LV function in Ang II mice. Ang II mice developed severe heart failure indicated by an impairment in systolic (EF, CO, dP/dt_{max}) (Fig. 7A–7C) and diastolic function (dP/dt_{min}, τ, LVEDP) (Fig. 7D–7F). CardAPs did not affect the heart rate in Ang II mice (control mice, 542 ± 21 beats per minutes [bpm]; Ang II mice, 487 ± 30 bpm; Ang II + CardAPs mice, 510 ± 20 bpm). CardAPs application ameliorated global LV function, as shown by a 1.5-fold ($p < .001$) increase in Ang II-decreased EF and improved the impaired LV systolic and diastolic function in Ang II-treated mice, as indicated by a 1.7-fold ($p < .05$) and 1.4-fold ($p < .05$) increase in CO and dP/dt_{max}, respectively; and a 1.3-fold ($p < .05$), 1.5-fold ($p < .001$),

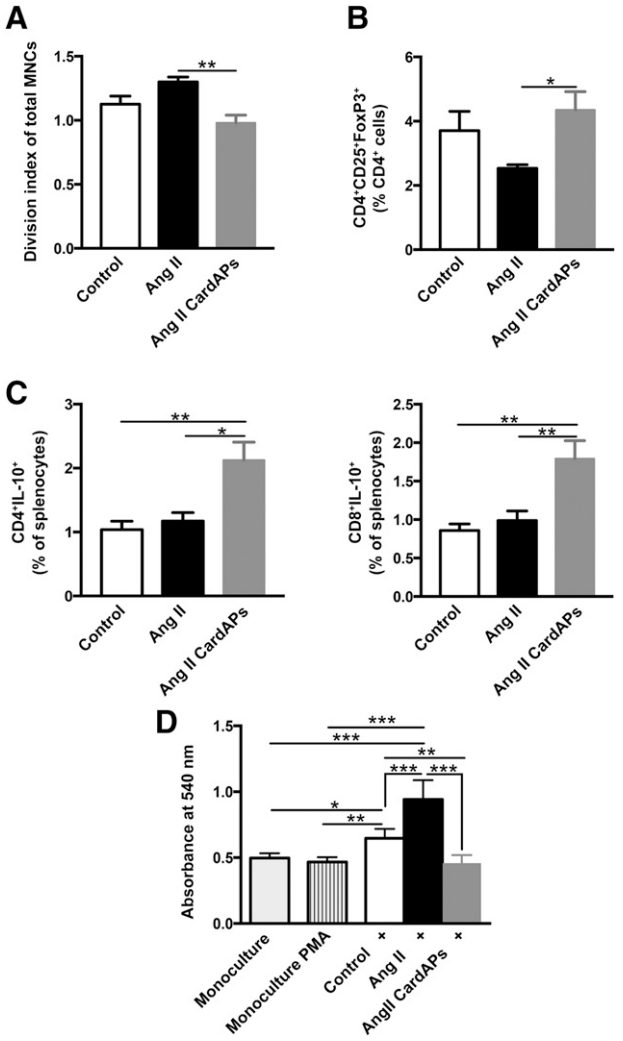

Figure 4. Endomyocardial biopsy specimen-derived cells exert prominent immunomodulatory effects in Ang II-treated mice that have an impact on collagen production in fibroblasts. **(A):** Bar graphs represent the mean ± SEM the division index of total MNCs, indicating the activation of MNCs in the spleen of control and Ang II-treated mice injected with phosphate-buffered saline (PBS) or CardAPs, respectively. $n = 5–6$ per group. **, $p < .01$. **(B):** $CD4^+CD25^+FoxP3^+$ T-regulator cells depicted as the percentage of CD4 cells in the spleen of control and Ang II-treated mice upon PBS or CardAPs application, respectively. $n = 4–5$ per group. *, $p < .05$. **(C):** IL-10-producing $CD4^+$ and $CD8^+$ T cells represented as the percentage of cells in the spleens of control and Ang II-treated mice injected with PBS or CardAPs, respectively. $n = 5–6$ per group. *, $p < .05$; **, $p < .01$. **(D):** The absorbance at 540 nm of Sirius Red-stained monocultured fibroblasts with or without 50 ng/ml PMA and 500 ng/ml ionomycin and cocultured with PMA/ionomycin-activated splenocytes of control, Ang II, and Ang II CardAPs mice, as indicated. $n = 6$ per group. *, $p < .05$; **, $p < .01$; and ***, $p < .001$. Abbreviations: Ang, angiotensin; CardAP, cardiac-derived adherent proliferating cell; IL, interleukin; MNC, mononuclear cell; PMA, phorbolmyristate acetate.

and 2.9-fold ($p < .0005$) decrease in dP/dt_{min}, τ, and LVEDP, respectively, compared with Ang II-treated mice.

Discussion

The salient finding of the present study is that CardAPs derived from endomyocardial biopsy specimens reduced Ang II-induced heart failure and cardiac remodeling by their antifibrotic, antihypertrophic, and immunomodulatory properties. The importance of Ang II in the induction of cardiac remodeling and subsequent heart failure is well established. ACE inhibitors and AT1R antagonists counteracting Ang II-mediated signaling are common drugs used to treat patients with heart failure. We recently isolated and identified novel cardiac biopsy-derived cells, CardAPs, which share several characteristics with MSCs, including their antiapoptotic [12], and immunomodulatory [12, 13] effects, and their low immunogenicity [13]. The well-described antifibrotic features of MSCs [24] have not been explored for CardAPs so far; direct antihypertrophic effects on cardiomyocytes also have not yet been identified for MSCs.

In this study, we demonstrate that CardAPs decreased cardiac dilatation, fibrosis, and hypertrophy in Ang II mice. In vitro, we showed that similar to their antiapoptotic [12], antiviral [12], and immunomodulatory [12, 13] properties, CardAPs exerted their antifibrotic and antihypertrophic effects in an NO- and IL-10-dependent manner. With respect to the antifibrotic features of CardAPs, this observation is supported by the finding that NO inhibits myocardial fibrosis through the suppression of cardiac fibroblast proliferation [30] and the activation of matrix metalloproteinases [30], as well as by the finding that endothelial nitric oxide synthase (eNOS)-deficient ($eNOS^{-/-}$) mice exhibit increased cardiac fibrosis [31]. The antifibrotic effects of IL-10 have been reported in different animal models of liver [32], airway [1], kidney [33], and cardiac fibrosis [34]. IL-10 has been shown to inhibit the proliferation and α-SMA expression of cultured neonatal cardiac fibroblasts [35] to attenuate extracellular matrix production [36], enhance extracellular matrix breakdown via upregulation of proteolytic enzymes [37], and suppress transforming growth factor-β1 expression [37], whereas IL-10 deficiency aggravates inflammation and fibrosis [38]. Oxidative stress plays an important role in the induction of collagen synthesis in cardiac fibroblasts [39] and in the transdifferentiation of cardiac fibroblasts to myofibroblasts [23], which are responsible for the disproportionate accumulation of extracellular matrix components [40]. Because NO [41] and IL-10 [42, 43] have antioxidative properties, we suggest that the antifibrotic effects of CardAPs are partly mediated via the antioxidative actions of NO and IL-10 released by CardAPs. In agreement with this hypothesis, CardAP supplementation to Ang II-stimulated cardiac fibroblasts reduced the collagen production and proliferation of cardiac fibroblasts, and their transdifferentiation into myofibroblasts, which was paralleled by a decrease in the Ang II-induced production of ROS in cardiac fibroblasts. In vivo, CardAP application resulted in a reduced phosphorylation state of the stress signaling mitogen activated protein kinase ERK, which is known to be a key player in Ang II-induced cardiac fibroblast proliferation [44].

Besides its profibrotic potential, ERK also induces hypertrophic responses in cardiomyocytes [45], which can be suppressed via NO [41]. This finding, together with the observations that both exogenous NO administration [46] and endogenous NO production [41] prevent cardiac hypertrophy and that $eNOS^{-/-}$ mice develop pressure overload-induced/age-related myocardial hypertrophy [47–50], supports our finding that the antihypertrophic actions of CardAPs also occurred in an NO-dependent manner. The IL-10 dependency of CardAPs' antihypertrophic actions is corroborated by the finding that IL-10 exerts antihypertrophic effects [51], which are reflected in IL-10's anti-inflammatory potential and its inhibitory effect on ERK signaling in cardiomyocytes [52].

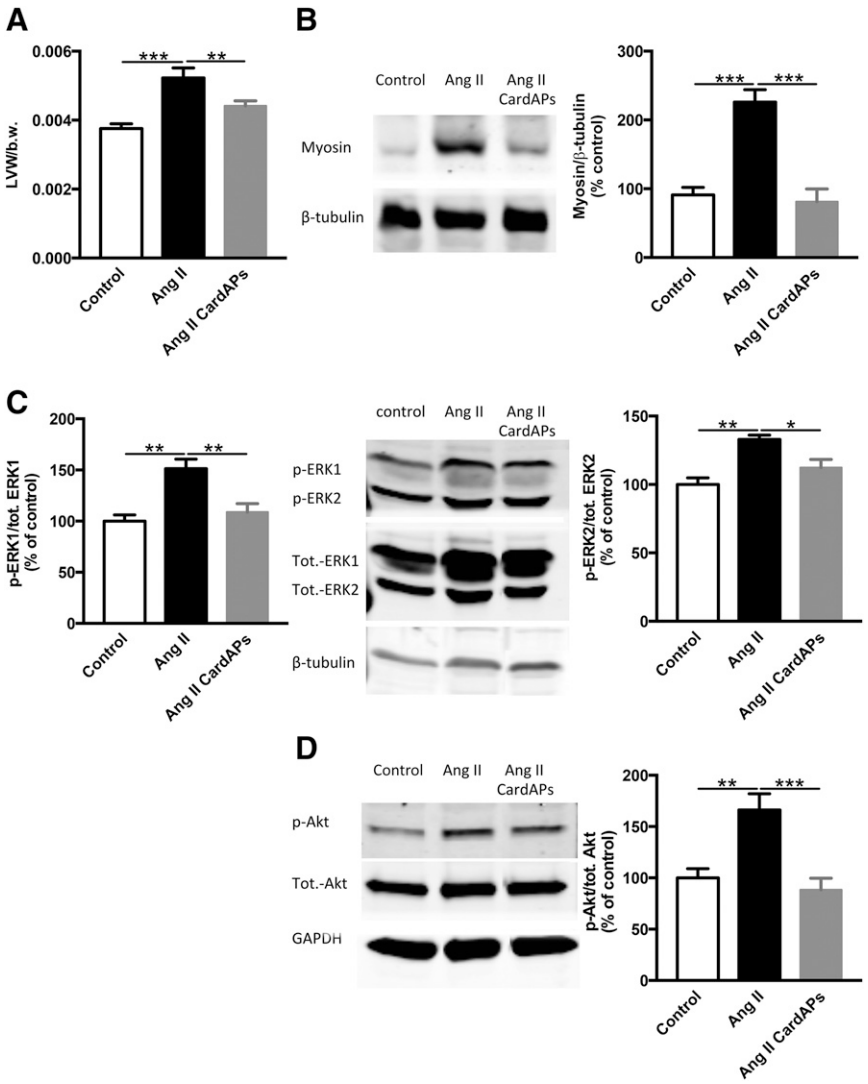

Figure 5. Endomyocardial biopsy specimen-derived cells reduced cardiac hypertrophy in Ang II-treated mice. **(A):** Bar graphs represent the mean ± SEM of the ratio of LVW to b.w. of control mice and Ang II-treated mice injected with phosphate-buffered saline (PBS) or CardAPs, as indicated. $n = 7–9$ per group. **, $p < .01$; ***, $p < .001$. **(B):** The ratio of myosin (heavy chain) to β-tubulin of control mice and Ang II-treated mice injected with PBS or CardAPs, as indicated. $n = 5$ per group. ***, $p < .001$. Left panel shows representative blots of myosin heavy chain and β-tubulin of the respective groups. **(C):** The ratio of p to tot. ERK1 and ERK2 of control mice and Ang II-treated mice injected with PBS or CardAPs, as indicated. $n = 4–5$ per group. **, $p < .01$. Middle panel shows representative blots of p-ERK1, p-ERK2, tot. ERK1, tot. ERK2, and β-tubulin. **(D):** The ratio of p to tot. Akt of control mice and Ang II-treated mice injected with PBS or CardAPs, as indicated. $n = 6–7$ per group. *, $p < .05$; **, $p < .01$. Left panel shows representative blots of p-Akt, tot. Akt, and GAPDH. Abbreviations: Ang, angiotensin; b.w., body weight; CardAP, cardiac-derived adherent proliferating cell; GADPH, glyceraldehyde-3-phosphate dehydrogenase; IL, interleukin; LVW, left ventricular weight; p, phosphorylated; tot., total.

Similarly, we demonstrated that CardAP application reduced the phosphorylation and activation of ERK in Ang II mice. The anti-hypertrophic effect of CardAPs was further indicated by a decrease in LV to body weight ratio and cardiac myosin (heavy chain) expression, as well as by the decline in Ang II-induced phosphorylation of the protein kinase B, Akt, which is another important mediator in Ang II-induced cardiomyocyte hypertrophy [4].

Because Ang II is also an important promoter of inflammation, which is a crucial trigger of cardiac fibrosis [29, 53] and hypertrophy [54], we further investigated the immunomodulatory actions of CardAPs in Ang II mice. CardAPs reduced the activation and proliferation of splenic MNCs and increased the percentage of CD4CD25FoxP3 Tregs in Ang II mice. Besides an upregulation of LV *IL-10* mRNA expression, CardAPs also raised the percentage of circulating CD4+IL10+ and CD8+IL10+ Tregs [28] in Ang II mice. Furthermore, splenocytes from Ang II+CardAPs mice induced less collagen production in fibroblasts compared with MNCs from Ang II mice. Given the anti-inflammatory [34] and direct antifibrotic potential of IL-10 [35], these data suggest that the CardAP-mediated immunomodulation, including the intrinsic increase in LV *IL-10* mRNA expression, as well as the induction of circulating CD4+IL-10+ and CD8+IL-10+ T cells, contributed to the reduction in cardiac fibrosis in Ang II+CardAPs compared with Ang II mice. This hypothesis is supported by the observation that transplantation of wild-type bone marrow MNCs, but not IL-10 knockout bone marrow MNCs, led to a decrease in collagen deposition in a myocardial infarction model [55]. These findings also further corroborate our hypothesis that besides the direct

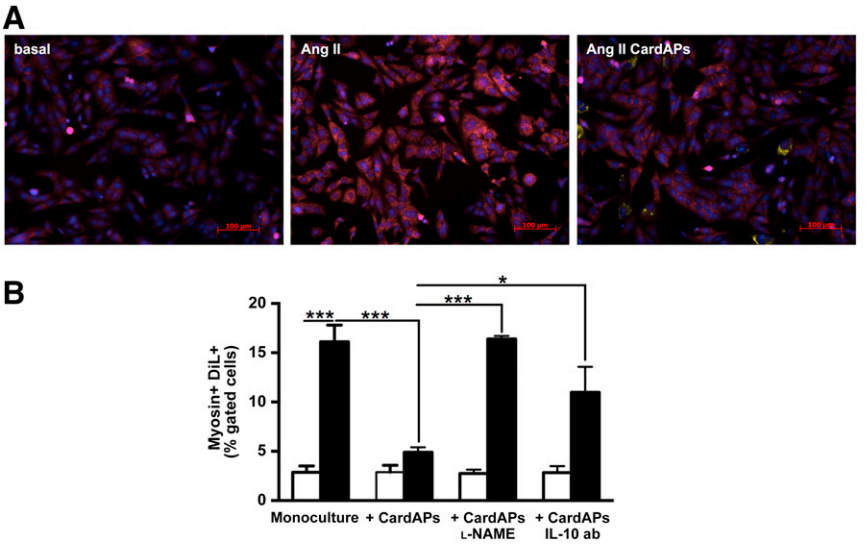

Figure 6. Endomyocardial biopsy specimen-derived cells reduce Ang II-induced HL-1 cardiomyocyte hypertrophy. **(A):** Representative pictures of Cy5-myosin-stained HL-1 cardiomyocytes (magnification, ×20) of basal, Ang II-stimulated HL-1 cells in the presence or absence of CardAPs, as indicated. **(B):** Bar graphs representing the mean ± SEM of $DiL^+/Myosin^+$ cells depicted as the percentage of gated cells of basal (open bars) or Ang II-treated (closed bars) HL-1 cells with or without untreated or L-NAME-treated CardAPs or CardAPs in the presence of 1 μg/ml anti-human IL-10 ab. $n = 4$ per group. *, $p < .05$; ***, $p < .001$. Abbreviations: ab, antibody; Ang, angiotensin; CardAP, cardiac-derived adherent proliferating cell; IL, interleukin; L-NAME, nitro-L-argininmethylesterhydrochloride.

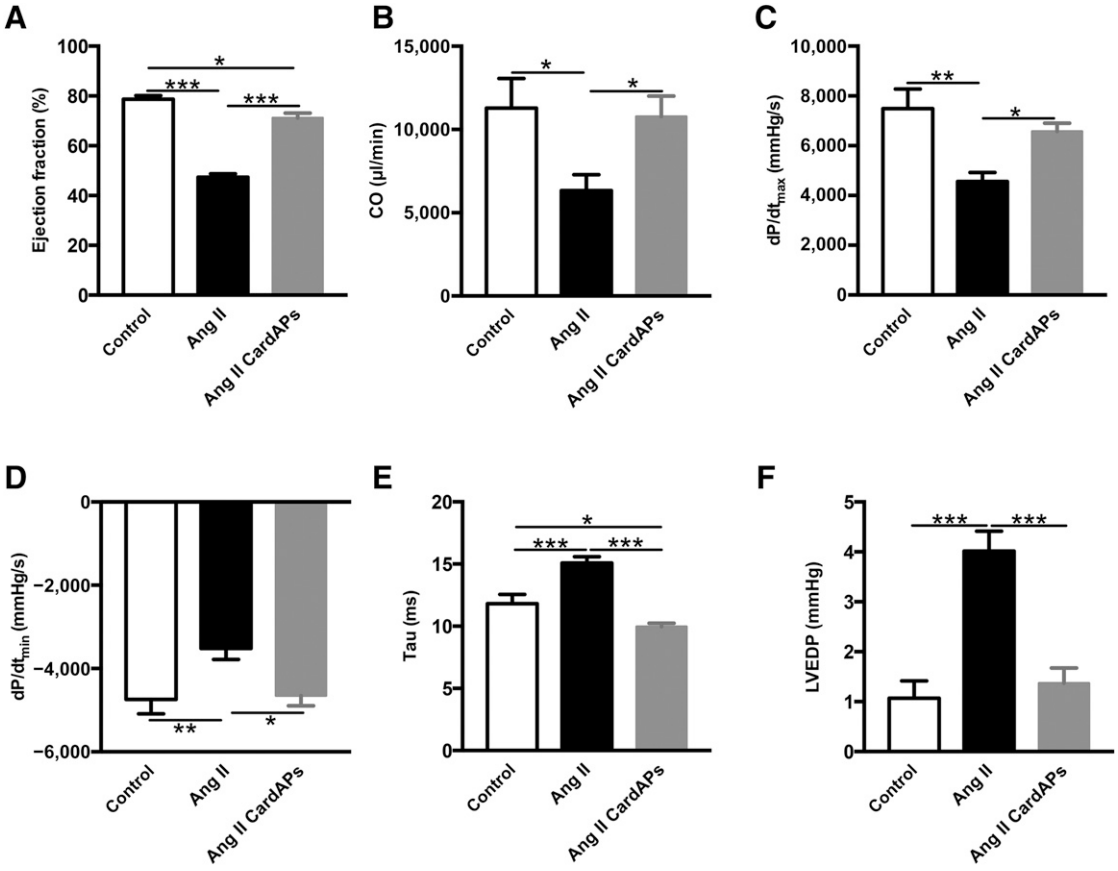

Figure 7. Endomyocardial biopsy specimen-derived cells improved left ventricular function in Ang II-treated mice. **(A–F):** Bar graphs representing percent ejection fraction **(A)**; CO **(B)**; dP/dt_{max} **(C**; dP/dt_{min} **(D)** Tau **(E)**; and LVEDP **(F)** of control mice and Ang II-treated mice injected with phosphate-buffered saline or CardAPs, as indicated. $n = 7$ per group. *, $p < .05$ versus Ang II; **, $p < .01$ versus Ang II; ***, $p < .001$ versus Ang II. Abbreviations: Ang, angiotensin; CardAP, cardiac-derived adherent proliferating cell; CO, cardiac output; dP/dt_{max}, left ventricle contractility; dP/dt_{min}, left ventricular pressure decrease; LVEDP, left ventricular end diastolic pressure.

cardioprotective effects of CardAPs, the extracardiac immunomodulatory effects of CardAPs also contribute to their mediated improvement in cardiac function [12] and suggest an involvement of the immunomodulatory effects of CardAPs in their antihypertrophic and antifibrotic actions.

Study Limitations

In the present study, the impact of CardAP application in Ang II mice was evaluated by hemodynamic measurements on the day of sacrifice, and by molecular biology, immunohistological, and flow cytometric evaluation of the characterization of underlying mechanisms. In view of translation of the findings to patients, further studies would be of relevance that evaluated the impact of CardAPs in Ang II mice, on long-term or in awake animals via telemetry, and also in larger animals. In this study, CardAPs from young adult mice with preserved ejection fraction were used. With respect to translation, further studies are needed that evaluate the potential of autologous CardAPs derived from heart failure patients on Ang II-induced cardiac remodeling. Nevertheless, CardAPs have low immunogenicity [13], indicating their potential allogenic use and thereby allowing the use of CardAPs from healthy donors.

Conclusion

CardAPs improved the Ang II-induced cardiac remodeling, involving their antifibrotic, antihypertrophic, and immunomodulatory properties.

Acknowledgments

We thank, in alphabetical order, Ulrike Fritz, Annika Koschel, Matthias Pippow, Kerstin Puhl, and Norbert G. Zingler for excellent technical assistance. We acknowledge the assistance of the Berlin-Brandenburg Center for Regenerative Therapies Flow Cytometry Lab. This study was supported by the Berlin-Brandenburg Center for Regenerative Therapies (BCRT; Bundesministerium für Bildung und Forschung – 0313911) to M.H., J.R., M.S., C.T., and S.V.L. by Deutsche Forschungsgemeinschaft funding through the BCRT and by the German Center for Cardiovascular Research (Deutsches Zentrum für Herz-Kreislauf-Forschung) to C.T.

Author Contributions

K.M.: administrative support, collection and/or assembly of data, data analysis and interpretation; S.V.L.: conception and design, administrative support, collection and/or assembly of data, data analysis and interpretation, manuscript writing; K.P. and I.M.: collection and/or assembly of data; F.S., M.H., and J.R.: provision of study material or patients; H.S.: establishment of Operetta method; M.S.: financial support, final approval of manuscript; C.T.: financial support, provision of study material or patients, final approval of manuscript.

Disclosure of Potential Conflicts of Interest

M.H. has uncompensated intellectual property rights. J.R. has uncompensated intellectual property rights. M.S. has uncompensated intellectual property rights and is an uncompensated shareholder. C.T. has compensated employment. The other authors indicated no potential conflicts of interest.

References

1 Wilson MS, Elnekave E, Mentink-Kane MM et al. IL-13Ralpha2 and IL-10 coordinately suppress airway inflammation, airway-hyperreactivity, and fibrosis in mice. J Clin Invest 2007;117:2941–2951.

2 Olson ER, Naugle JE, Zhang X et al. Inhibition of cardiac fibroblast proliferation and myofibroblast differentiation by resveratrol. Am J Physiol Heart Circ Physiol 2005;288: H1131–H1138.

3 Kvakan H, Kleinewietfeld M, Qadri F et al. Regulatory T cells ameliorate angiotensin II-induced cardiac damage. Circulation 2009;119:2904–2912.

4 Hingtgen SD, Tian X, Yang J et al. Nox2-containing NADPH oxidase and Akt activation play a key role in angiotensin II-induced cardiomyocyte hypertrophy. Physiol Genomics 2006; 26:180–191.

5 Nakamura Y, Yoshiyama M, Omura T et al. Beneficial effects of combination of ACE inhibitor and angiotensin II type 1 receptor blocker on cardiac remodeling in rat myocardial infarction. Cardiovasc Res 2003;57:48–54.

6 Kim S, Yoshiyama M, Izumi Y et al. Effects of combination of ACE inhibitor and angiotensin receptor blocker on cardiac remodeling, cardiac function, and survival in rat heart failure. Circulation 2001;103:148–154.

7 Pfeffer MA, Swedberg K, Granger CB et al. Effects of candesartan on mortality and morbidity in patients with chronic heart failure: The CHARM-Overall programme. Lancet 2003;362: 759–766.

8 Van Linthout S, Savvatis K, Miteva K et al. Mesenchymal stem cells improve murine acute Coxsackievirus B3-induced myocarditis. Eur Heart J 2011;32:2168–2178.

9 Sorrell JM, Baber MA, Caplan AI. Influence of adult mesenchymal stem cells on in vitro vascular formation. Tissue Eng Part A 2009;15: 1751–1761.

10 Haag M, Van Linthout S, Schröder SE et al. Endomyocardial biopsy derived adherent proliferating cells - a potential cell source for cardiac tissue engineering. J Cell Biochem 2010;109: 564–575.

11 Choi YH, Saric T, Nasseri B et al. Cardiac cell therapies: The next generation. Cardiovasc Ther 2011;29:2–16.

12 Miteva K, Haag M, Peng J et al. Human cardiac-derived adherent proliferating cells reduce murine acute Coxsackievirus B3-induced myocarditis. PLoS One 2011;6:e28513.

13 Haag M, Stolk M, Ringe J et al. Immune attributes of cardiac-derived adherent proliferating (CAP) cells in cardiac therapy. J Tissue Eng Regen Med 2013;7:362–370.

14 Tschöpe C, Kherad B, Schultheiss HP. How to perform an endomyocardial biopsy? Turk Kardiyol Dern Ars 2015;43:572–575.

15 Tschöpe C, Bock CT, Kasner M et al. High prevalence of cardiac parvovirus B19 infection in patients with isolated left ventricular diastolic dysfunction. Circulation 2005;111: 879–886.

16 Westermann D, Becher PM, Lindner D et al. Selective PDE5A inhibition with sildenafil rescues left ventricular dysfunction, inflammatory immune response and cardiac remodeling in angiotensin II-induced heart failure in vivo. Basic Res Cardiol 2012;107:308.

17 McBride C, Gaupp D, Phinney DG. Quantifying levels of transplanted murine and human mesenchymal stem cells in vivo by real-time PCR. Cytotherapy 2003;5:7–18.

18 Van Linthout S, Lusky M, Collen D et al. Persistent hepatic expression of human apo A-I after transfer with a helper-virus independent adenoviral vector. Gene Ther 2002;9: 1520–1528.

19 De Geest BR, Van Linthout SA, Collen D. Humoral immune response in mice against a circulating antigen induced by adenoviral transfer is strictly dependent on expression in antigen-presenting cells. Blood 2003;101: 2551–2556.

20 Savvatis K, van Linthout S, Miteva K et al. Mesenchymal stromal cells but not cardiac fibroblasts exert beneficial systemic immunomodulatory effects in experimental myocarditis. PLoS One 2012;7:e41047.

21 Spillmann F, Miteva K, Pieske B et al. High-density lipoproteins reduce endothelial-to-mesenchymal transition. Arterioscler Thromb Vasc Biol 2015;35:1774–1777.

22 Staal EM, Baan J, Jukema JW et al. Assessment of parallel conductance for the transcardiac conductance method: Can we use the hypertonic saline method with pulmonary artery injections? Physiol Meas 2004;25:565–576.

23 Shen WL, Gao PJ, Che ZQ et al. NAD(P)H oxidase-derived reactive oxygen species regulate angiotensin-II induced adventitial fibroblast phenotypic differentiation. Biochem Biophys Res Commun 2006;339:337–343.

24 Mias C, Lairez O, Trouche E et al. Mesenchymal stem cells promote matrix metalloproteinase secretion by cardiac fibroblasts and reduce cardiac ventricular fibrosis after myocardial infarction. STEM CELLS 2009;27:2734–2743.

25 Van Linthout S, Spillmann F, Lorenz M et al. Vascular-protective effects of high-density lipoprotein include the downregulation of the angiotensin II type 1 receptor. Hypertension 2009;53:682–687.

26 Aragno M, Mastrocola R, Alloatti G et al. Oxidative stress triggers cardiac fibrosis in the heart of diabetic rats. Endocrinology 2008; 149:380–388.

27 Benigni A, Cassis P, Remuzzi G. Angiotensin II revisited: New roles in inflammation, immunology and aging. EMBO Mol Med 2010;2: 247–257.

28 Noble A, Giorgini A, Leggat JA. Cytokine-induced IL-10-secreting CD8 T cells represent a phenotypically distinct suppressor T-cell lineage. Blood 2006;107:4475–4483.

29 Van Linthout S, Miteva K, Tschöpe C. Crosstalk between fibroblasts and inflammatory cells. Cardiovasc Res 2014;102:258–269.

30 Kurisu S, Ozono R, Oshima T et al. Cardiac angiotensin II type 2 receptor activates the kinin/NO system and inhibits fibrosis. Hypertension 2003;41:99–107.

31 O'Riordan E, Mendelev N, Patschan S et al. Chronic NOS inhibition actuates endothelial-mesenchymal transformation. Am J Physiol Heart Circ Physiol 2007;292:H285–H294.

32 Lan L, Chen Y, Sun C et al. Transplantation of bone marrow-derived hepatocyte stem cells transduced with adenovirus-mediated IL-10 gene reverses liver fibrosis in rats. Transpl Int 2008;21:581–592.

33 Mu W, Ouyang X, Agarwal A et al. IL-10 suppresses chemokines, inflammation, and fibrosis in a model of chronic renal disease. J Am Soc Nephrol 2005;16:3651–3660.

34 Krishnamurthy P, Rajasingh J, Lambers E et al. IL-10 inhibits inflammation and attenuates left ventricular remodeling after myocardial infarction via activation of STAT3 and suppression of HuR. Circ Res 2009;104:e9–e18.

35 Li Z, Wei H, Deng L et al. Expression and secretion of interleukin-1β, tumour necrosis factor-α and interleukin-10 by hypoxia- and serum-deprivation-stimulated mesenchymal stem cells. FEBS J 2010;277:3688–3698.

36 Occleston NL, O'Kane S, Goldspink N et al. New therapeutics for the prevention and reduction of scarring. Drug Discov Today 2008;13: 973–981.

37 Yamamoto T, Eckes B, Krieg T. Effect of interleukin-10 on the gene expression of type I collagen, fibronectin, and decorin in human skin fibroblasts: Differential regulation by transforming growth factor-beta and monocyte chemoattractant protein-1. Biochem Biophys Res Commun 2001;281:200–205.

38 Jin Y, Liu R, Xie J et al. Interleukin-10 deficiency aggravates kidney inflammation and fibrosis in the unilateral ureteral obstruction mouse model. Lab Invest 2013;93:801–811.

39 Siwik DA, Pagano PJ, Colucci WS. Oxidative stress regulates collagen synthesis and matrix metalloproteinase activity in cardiac fibroblasts. Am J Physiol Cell Physiol 2001;280: C53–C60.

40 Swaney JS, Roth DM, Olson ER et al. Inhibition of cardiac myofibroblast formation and collagen synthesis by activation and overexpression of adenylyl cyclase. Proc Natl Acad Sci USA 2005;102:437–442.

41 Cheng TH, Shih NL, Chen SY et al. Nitric oxide inhibits endothelin-1-induced cardiomyocyte hypertrophy through cGMP-mediated suppression of extracellular-signal regulated kinase phosphorylation. Mol Pharmacol 2005;68: 1183–1192.

42 Gunnett CA, Heistad DD, Berg DJ et al. IL-10 deficiency increases superoxide and endothelial dysfunction during inflammation. Am J Physiol Heart Circ Physiol 2000;279: H1555–H1562.

43 Kaur K, Sharma AK, Dhingra S et al. Interplay of TNF-alpha and IL-10 in regulating oxidative stress in isolated adult cardiac myocytes. J Mol Cell Cardiol 2006;41:1023–1030.

44 Olson ER, Shamhart PE, Naugle JE et al. Angiotensin II-induced extracellular signal-regulated kinase 1/2 activation is mediated by protein kinase Cdelta and intracellular calcium in adult rat cardiac fibroblasts. Hypertension 2008;51:704–711.

45 Molkentin JD. Calcineurin-NFAT signaling regulates the cardiac hypertrophic response in coordination with the MAPKs. Cardiovasc Res 2004;63:467–475.

46 Calderone A, Thaik CM, Takahashi N et al. Nitric oxide, atrial natriuretic peptide, and cyclic GMP inhibit the growth-promoting effects of norepinephrine in cardiac myocytes and fibroblasts. J Clin Invest 1998;101:812–818.

47 Ichinose F, Bloch KD, Wu JC et al. Pressure overload-induced LV hypertrophy and dysfunction in mice are exacerbated by congenital NOS3 deficiency. Am J Physiol Heart Circ Physiol 2004;286:H1070–H1075.

48 Ruetten H, Dimmeler S, Gehring D et al. Concentric left ventricular remodeling in endothelial nitric oxide synthase knockout mice by chronic pressure overload. Cardiovasc Res 2005;66:444–453.

49 Buys ES, Raher MJ, Blake SL et al. Cardiomyocyte-restricted restoration of nitric oxide synthase 3 attenuates left ventricular remodeling after chronic pressure overload. Am J Physiol Heart Circ Physiol 2007;293: H620–H627.

50 Barouch LA, Harrison RW, Skaf MW et al. Nitric oxide regulates the heart by spatial confinement of nitric oxide synthase isoforms. Nature 2002;416:337–339.

51 Nonaka-Sarukawa M, Okada T, Ito T et al. Adeno-associated virus vector-mediated systemic interleukin-10 expression ameliorates hypertensive organ damage in Dahl salt-sensitive rats. J Gene Med 2008;10:368–374.

52 Hovsepian E, Penas F, Siffo S et al. IL-10 inhibits the NF-κB and ERK/MAPK-mediated production of pro-inflammatory mediators by up-regulation of SOCS-3 in *Trypanosoma cruzi*-infected cardiomyocytes. PLoS One 2013;8: e79445.

53 Westermann D, Lindner D, Kasner M et al. Cardiac inflammation contributes to changes in the extracellular matrix in patients with heart failure and normal ejection fraction. Circ Heart Fail 2011;4:44–52.

54 Masiha S, Sundström J, Lind L. Inflammatory markers are associated with left ventricular hypertrophy and diastolic dysfunction in a population-based sample of elderly men and women. J Hum Hypertens 2013;27:13–17.

55 Burchfield JS, Iwasaki M, Koyanagi M et al. Interleukin-10 from transplanted bone marrow mononuclear cells contributes to cardiac protection after myocardial infarction. Circ Res 2008;103:203–211.

